Controlling Spatiotemporal Patterns on a Catalytic Wafer

F. Qin, E. E. Wolf, and H.-C. Chang
Department of Chemical Engineering, University of Notre Dame, Notre Dame, Indiana 46556
(Received 6 July 1993)

A video-feedback control experiment which successfully suppresses chaotic temporal fluctuations of thermal patterns on a catalytic wafer is reported. A Karhunen-Loeve scheme is used to identify the dominant spatial structures from video imaging and estimate the low-dimensional temporal dynamics. The projected dynamics shows that the spatiotemporal chaos is due to an intermittent chaotic attractor near a homoclinic orbit. The control strategy is then simply to stabilize the hyperbolic fixed point attached to the homoclinic orbit with a local model feedback control.

PACS numbers: 05.45.+b

Ott, Grebogi, and Yorke [1] recently suggested that chaotic behavior can be suppressed if one can utilize feedback control to stabilize an arbitrary unstable periodic orbit or fixed point of the system. The approach is to force the flow to converge to the stable manifold (eigenvector) of the desired "set point"—a periodic orbit or a fixed point. To estimate the unstable eigenvector such that the flow will have no projection in its direction after the controller is activated, a delayed-embedding technique is used to estimate the linear dynamics near the set point. Their subsequent feedback control technique is not dissimilar to the classical pole-placement and dead-beat control strategies. This chaos control scheme was successfully implemented to reduce chaotic behavior to periodic oscillations in a buckling ribbon [2], in cardiac arrhythmias [3], and in a Belousov-Zhabotinsky reaction [4]. However, the original chaos control strategies to stabilize a periodic orbit or a fixed point are designed for "lumped" systems with no spatial dependence or for effectively lumped systems with simple and regular spatial structures. For example in the buckling ribbon experiment, even though the temporal dynamics is chaotic, the only excited spatial mode is a simple buckling mode. Most realistic systems are distributed ones, however, which exhibit spatiotemporal dynamics with pronounced and complex spatial structures. The control of such spatiotemporal dynamics remains largely an open problem. Potentially the most important example is the stabilization of plasma instabilities for better plasma confinement in tokamak fusion machines [5]. There are two reasons why successful control of distributed systems remains elusive and both are related to their infinite dimensionality. It is difficult to identify the partial differential equations that describe their spatiotemporal dynamics (lumped systems are described by finite-dimensional ordinary differential equations) and it is difficult to control the infinite number of modes. In plasma control, efforts to stabilize a particular mode often destabilize other modes. In some rare examples where spatiotemporal chaos has been stabilized, typically only one or two eigenvalues in the infinite-dimensional spectrum are unstable. McDermott and Chang [6] used a proportional controller to stabilize the fixed point of a distributed autothermal reactor and Singer, Wang, and Bau [7] used a bang-bang controller to stabilize a chaotic thermal convection loop. The extensive modeling effort by McDermott and Chang for the first system shows that the fixed point has a lone unstable eigenvalue and the convective loop, which is described by the Lorenz equation under idealized conditions, can be adequately described by a three-dimensional dynamical system. Even though these specific distributed systems are more amenable to control stabilization, it is difficult *a priori* to determine whether the unstable spectrum of a potential set point in a spatially distributed system is low dimensional. In fact, even the unstable fixed point or periodic orbit, about which linearization is carried out to obtain the spectrum, is difficult to determine *a priori*. This requires an elaborate nonlinear model identification scheme for spatiotemporal dynamics.

The identification problem associated with a distributed system is seen when one applies the delayed-embedding technique to a time series from a single point sensor. Chen, Wolf, and Chang [8] have recently examined the viability of this identification scheme for spatiotemporal chaos exhibited by thermal hot spots on a catalytic wafer. Such thermal patterns have been shown by Wolf and his co-workers to exhibit very interesting spatiotemporal dynamics using IR thermography and other techniques [9]. In an effectively lumped system like the buckling ribbon experiments, the spatial structure is so simple that time series taken from sensors located at arbitrary locations on the ribbon would yield identical temporal dynamics. The rich spatial structures of the hot spot dynamics described later in this Letter were shown to render the delayed-embedding technique inaccurate. Time series from different locations on the wafer yield different Lyapunov exponents and the leading exponent does not converge with respect to the embedding dimension [8]. It is hence clear that distributed dynamics cannot be captured with a single probe in general and multiple sensors over the entire domain must be used. For moving structures with steep spatial gradients, fine spatial resolution over a large domain is required and dense two-dimensional (or even three-dimensional) sensor arrays, such as those offered by video imaging in our experiment, would be required. The extension from a zero-

0031-9007/94/72(11)/1459(4)$06.00

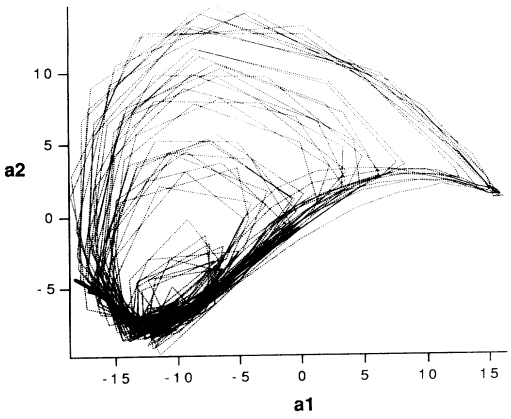

FIG. 1. Projected dynamics from the video tape in the phase space spanned by the first two Karhunen-Loeve modes. The fixed point $\mathbf{a}^*$ and its eigenvectors $\hat{\mathbf{e}}_1$ and $\hat{\mathbf{e}}_2$ are shown.

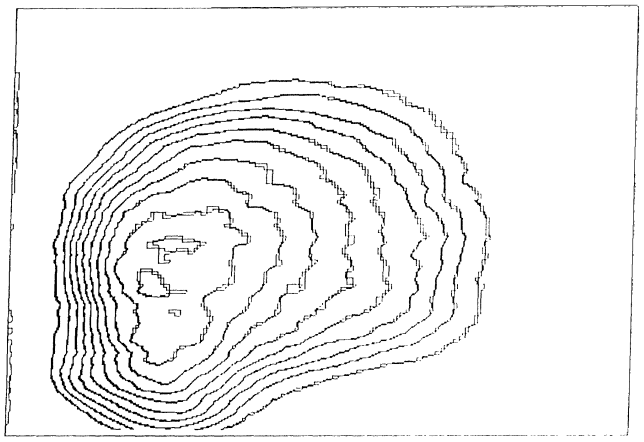

FIG. 2. The temperature field image on the wafer corresponding to the fixed point of Fig. 1. Each curve corresponds to an isotherm and the isotherms are 10°C apart with the maximum temperature at about 150°C. The feed comes in from the lower left corner.

dimension sensor to two- or three-dimensional distributed sensors immediately implies a tremendous increase in data points—a total of 105×68 pixels exist for each frame of our video and each pixel can represent eight possible colors. This implies that the construction of an appropriate dynamical system, or even deciphering basic dynamic characteristics like the Lyapunov exponent, would be difficult; not to mention the actual application of feedback control with so many output variables. Even the on-line, real-time processing of the data during feedback control is a significant hurdle. It is clear that some form of data reduction is required.

If the dynamics is dominated by many nearly independent spatial modes, which interact intermittently with little spatial coherence, the spatiotemporal dynamics of the distributed system is then truly infinite dimensional, or nearly so. There is then little hope of describing it with a low-dimensional dynamical system. Data reduction of the measurements from the distributed sensors and control stabilization are doomed to fail. There is, however, some distributed systems which exhibit low-dimensional temporal dynamics. Their spatiotemporal behavior is typically dominated by a few distinct coherent structures. Because of the spatial migration of these structures, the low-dimensional dynamics cannot be deciphered from the delayed-embedding analysis of a single-probe measurement. However, a new Karhunen-Loeve technique [10] can now extract it from distributed measurements. In our earlier experiment [8], we have used this technique to show that the spatiotemporal dynamics of hot spots on a Rh/SiO_2 catalytic wafer for CO oxidation can be interpreted as a Melnikov-type bifurcation of a homoclinic orbit in a five-dimensional phase space. The wafer is housed in a reactor and the gas reactants, CO and O_2, are fed into the reactor from a single feed. The effluent gas exits diagonally from the feed and is sent to an infrared analyzer which records continuously the product CO_2 concentration. There is an infrared transparent CaF_2 window to the reactor and the temperature field on the wafer is monitored by an AGA 782 infrared camera [9]. Each frame of the video tape can be accurately represented by five coefficients of the Karhunen-Loeve expansion. This corresponds to a data-reduction ratio of 1428 to 1: The projected trajectory from the video tape is shown in the phase space of the first two coefficients in Fig. 1. The intermittent departure from the unstable fixed point $\mathbf{a}^*$ is evident. The temperature field corresponding to the fixed point shown in Fig. 2 has a hot spot near the gas feed. The hot spot departs from this position intermittently and takes a tortuous path around the wafer before returning to the position in Fig. 2. Its wandering path, especially near the fixed point, is perturbed by high-frequency and localized fluctuations which are captured by the higher modes in the Karhunen-Loeve expansion. These are the fluctuations required to render a homoclinic orbit into a strange attractor according to the Melnikov mechanism (see Ref. [8] for more details).

We begin by decomposing the pixel signal $z(i,j)(t)$ of the video snapshots by the empirical eigenfunctions $\psi(i,j)$ from the Karhunen-Loeve technique [11]

$$z(i,j)(t)=\sum_{m=1}^{M} a_m(t)\psi(i,j) \tag{1}$$

and obtain the open-loop dynamical system

$$\dot{\mathbf{a}}=\mathbf{f}(\mathbf{a};u)\,, \tag{2}$$

where the overdot denotes time derivative. The scalar u is the input or manipulated variable which, in our experiments, corresponds to either the CO feed rate or the ratio of the CO and O_2 feed rates. In the experiments, both flow rates are controlled by mass flow meters. The scalar u is reduced such that $u=0$ corresponds to the nominal (open-loop) flow rate. Because the Karhunen-Loeve

method is so efficient in capturing the low-dimensional dynamics, we find that $M < 5$ is sufficient in all our experiments to ensure 90% resolution [11]. Since the Karhunen-Loeve technique is based on the time-averaged video frame, which does not necessarily represent the unstable steady state of the system, $\mathbf{a}=\mathbf{0}$ is not a fixed point of (2). We can hence estimate the fixed point $\mathbf{a}^*$ of the map (2) by a Newton-Raphson iteration with the local tangent map approximation of (2) constructed from the nearest neighbors [8]. However, for the projected trajectory shown in Fig. 1, the location of the fixed point can be determined accurately by inspection. The map is then reduced with respect to $\mathbf{a}^*$,

$$\dot{\mathbf{c}}=\mathbf{A}\mathbf{c}+\mathbf{B}u+\mathbf{g}(\mathbf{c};u), \tag{3}$$

where $\mathbf{c}=\mathbf{a}-\mathbf{a}^*$ and $\mathbf{g}(\mathbf{c})$ represents the nonlinear part of the map, $\mathbf{g}(\mathbf{0};0)=\mathbf{0}$. The estimation of $\mathbf{f}$ and $\mathbf{g}$ can be carried out using a singular-value decomposition technique [11]. However, because our chaotic attractor originates from a homoclinic orbit attached to a hyperbolic fixed point, we can suppress the spatiotemporal chaos by simply stabilizing the fixed point using linear feedback. For modal feedback control [11], this requires only information on the Jacobian $\mathbf{A}=\partial\mathbf{f}/\partial\mathbf{a}(\mathbf{a}^*,0)$, provided the system is linearly feedback stabilizable, which will be defined more explicitly later. The vector $\mathbf{B}=\partial\mathbf{f}/\partial u(\mathbf{a}^*, 0)$ also does not have to be estimated. Consequently, the stable and unstable eigenvectors of the fixed point, which can be obtained by inspection from Fig. 1 or from a more elaborate estimation scheme [11], and the two eigenvalues, which can be easily estimated from $\mathbf{a}(t)$, yield all the required information on $\mathbf{A}$, and explicit information of $\mathbf{f}$ and its derivatives is not necessary to obtain $\mathbf{A}$. After a similarity transform $\mathbf{c}=\mathbf{T}\mathbf{z}$ where the columns of $\mathbf{T}$ are simply the eigenvectors of $\mathbf{A}$ shown in Fig. 1, we obtain the canonical form

$$\dot{\mathbf{z}}=\mathbf{\Lambda}\mathbf{z}+\mathbf{D}u\,, \tag{4}$$

where $\mathbf{\Lambda}$ is a diagonal matrix containing the eigenvalues and the vector $\mathbf{D}$ is simply $\mathbf{T}^{-1}\mathbf{B}$. From Fig. 1, it is clear that only the first eigenvalue λ_1 in $\mathbf{\Lambda}$ is in the right half of the complex plane.

Our strategy for suppressing the chaotic behavior is to use feedback control to stabilize λ_1, as first suggested by Ott, Grebogi, and Yorke [1]. We shall, however, use a different continuous time, modal feedback law. It is clear from (4) that the lone unstable mode can be stabilized if one chooses

$$u(t)=-kz_1=-k\mathbf{c}\cdot\hat{\mathbf{e}}_1=-k(\mathbf{a}-\mathbf{a}^*)\cdot\hat{\mathbf{e}}_1\,, \tag{5}$$

where k is the controller gain and $\hat{\mathbf{e}}_1$ is the first left (adjoint) eigenvector of $\mathbf{A}$ or the first row of $\mathbf{T}^{-1}$. As mentioned before, $\mathbf{T}$, $\mathbf{T}^{-1}$, and hence $\hat{\mathbf{e}}_1$ can be easily estimated from Fig. 1. With this single-mode feeback, the closed-loop eigenvalues can be shown to be $\mu_1=\lambda_1-kD_1$ and $\mu_2=\lambda_2$ such that only the first mode is affected by

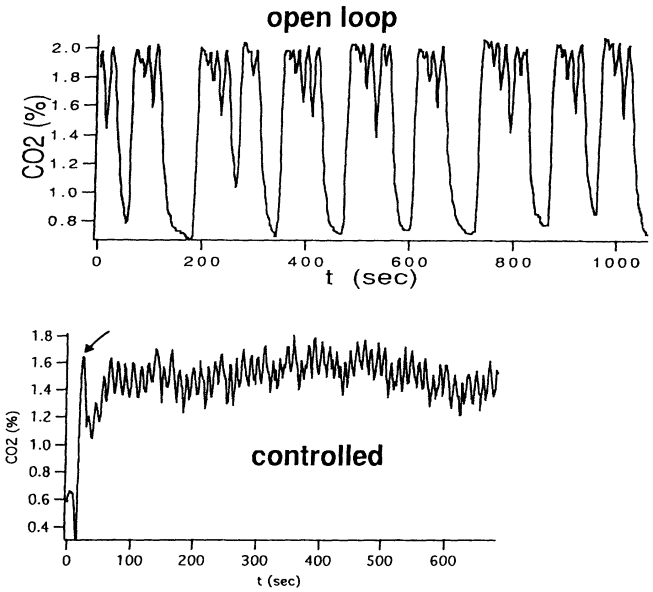

FIG. 3. Suppression of chaotic fluctuation by modal feedback. The controller is turned on at the point marked by the arrow.

feedback. The sign of the controller gain can then be determined empirically such that $kD_1>0$ and the first mode is stabilized. Hence, linear stabilizability corresponds to a nonzero D_1 in our case, and the vector $\mathbf{D}$ does not need to be estimated since $kD_1>0$ can be ensured by a single experiment. The decoupling of the stable second mode (in fact, all other stable modes) exists only if $\mathbf{a}^*$ and $\hat{\mathbf{e}}_1$ in (7) are known exactly. Estimation error will produce some coupling but, as long as k is not too large, the stable spectrum will not be destabilized [11]. Some tuning of k is hence necessary. The projection $a_m(t)=\langle z(i,j),\Psi_m(i,j)\rangle$ in the feedback law is the bottleneck step in the feedback scheme. It involves $(105\times6)^2\times M$ operations per time step after the empirical eigenfunctions $\Psi_m(i,j)$ have been determined and stored on-line. Our present frame-grabber software requires about 2 sec for computation and storage. The flow valve actuator contributes a 2 sec delay and the time required for the reactants to reach the reactor from the valve is about 1 sec. This adds to about a 5 sec delay. Although this is still small compared to the 100 sec characteristic time for the uncontrolled system seen in Fig. 3, it is significant to induce some fast jitters to the closed-loop dynamics. In Fig. 3, the suppression of the periodic and chaotic hot spot dynamics by feedback control as seen at the effluent CO_2 concentration is shown. A small-amplitude oscillation with a small period close to the delay is seen after the controller is activated to manipulate the CO feed rate according to (5). Consequently, the delay has prevented us from completely stabilizing the fixed point. Nevertheless, it has achieved significant suppression of the temporal fluctuation. We have verified that the delay is responsible for the small fluctuation by introducing additional delay

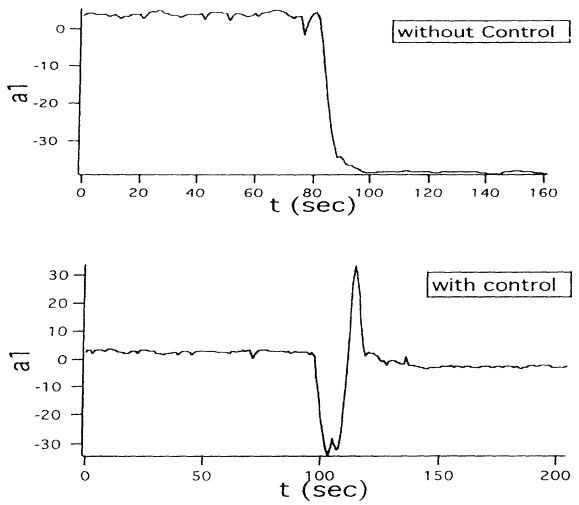

FIG. 4. Prevention of extinction by feedback control due to a large pulse perturbation of the oxygen feed.

to the feedback and the amplitude of the fluctuation increases monotonically as the delay increases. The small-amplitude closed-loop fluctuations ($\sim 0.2\%$ CO_2) are smaller than the chaotic ones without controller ($\sim 1.2\%$ CO_2). The hot spot wobbles around the position shown in Fig. 2 but does not take large excursions away from it as in the uncontrolled case. There is some steady-state offset as the temperature of the controlled hot spot is lower than that in Fig. 2. This explains the lower mean exit CO_2 concentration ($\sim 1.6\%$) with the controller on relative to the 2.0% without control when the hot spot is at the position in Fig. 2.

Many highly exothermic spatially distributed reactions, like flame combustion, etc., exhibit ignition and extinction corresponding to two coexisting, locally stable fixed points with finite domains of attraction. A sufficiently large perturbation can then cause the system to shift from one fixed point to another with typically undesirable practical consequences. Such extinction-ignition phenomena are related to the hysteresis behavior if a system parameter is varied as a bifurcation parameter. Instead of chaotic spatiotemporal dynamics, our system also exhibits ignition and extinction as a stationary hot spot will ignite or extinguish in response to a large but transient disturbance as shown in Fig. 4. We have also successfully used the feedback law of (5) to suppress this behavior such that the system returns to the original state (the ignited state in Fig. 4) after some transient. In this case, the control delay simply introduces an insignificant extension (~ 5 sec) of the transient period without causing any fluctuation. This is because, unlike chaos control of Fig. 3, the fixed point is stable for the uncontrolled system and the controller simply enlarges its domain of attraction. The other fixed point can sometimes be eliminated entirely by feedback.

In conclusion, we are able to experimentally suppress low-dimensional spatiotemporal dynamics of a distributed thermal hot spot system by using modal feedback control. This technique requires estimating the local dynamics near a fixed point via a Karhunen-Loeve analysis of the IR video images and by using the dynamics in a video feedback control scheme. We are assisted by the fact that the spatiotemporal chaos is related to a homoclinic orbit which, in turn, is connected to a hyperbolic fixed point with only one unstable eigenvalue. Suppressing the chaotic behavior hence involves only stabilizing the fixed point. The performance of our feedback control scheme can be further improved if we can diminish delay in the controller action. This can be achieved with a faster scan converter in the video camera, or more likely, with a faster algorithm to carry out projection of the video images onto the coordinates spanned by the empirical eigenfunctions.

This work is supported by NSF under Grants No. CTS-9112977 and No. CTS-92-00210. We are also grateful to C. C. Chen and Professor C. Hwang for their contributions to the initial experiments and writing the computer software.

[1] E. Ott, C. Grebogi, and J. A. Yorke, Phys. Rev. Lett. **64**, 1196 (1990).
[2] W. L. Ditto, S. N. Rauseo, and M. L. Spano, Phys. Rev. Lett. **65**, 3211 (1990).
[3] A. Garfinkel, M. L. Spano, W. L. Ditto, and J. N. Weiss, Science **257**, 1230 (1992).
[4] V. Petrov, V. Gaspar, J. Masere, and K. Showalter, Nature (London) **361**, 140 (1993).
[5] P. Tham and A. K. Sen, Phys. Rev. A **46**, 4520 (1992).
[6] P. E. McDermott and H.-C. Chang, Chem. Eng. Sci. **38**, 1347 (1984); **40**, 1355 (1985).
[7] J. Singer, Y.-Z. Wang, and H. H. Bau, Phys. Rev. Lett. **66**, 1123 (1991).
[8] C.-C. Chen, E. E. Wolf, and H.-C. Chang, J. Phys. Chem. **97**, 1055 (1993).
[9] D. J. Kaul and E. E. Wolf, J. Catal. **89**, 348 (1984); J. Kellow and E. E. Wolf, Chem. Eng. Sci. **45**, 2597 (1990); AIChE J. **37**, 1944 (1991).
[10] M. Loeve, *Probability Theory* (Van Nostrand, Princeton, 1955); L. Sirovich, Physica (Amsterdam) **37D**, 126 (1989).
[11] C.-C. Chen and H.-C. Chang, AIChE J. **38**, 1461 (1992).

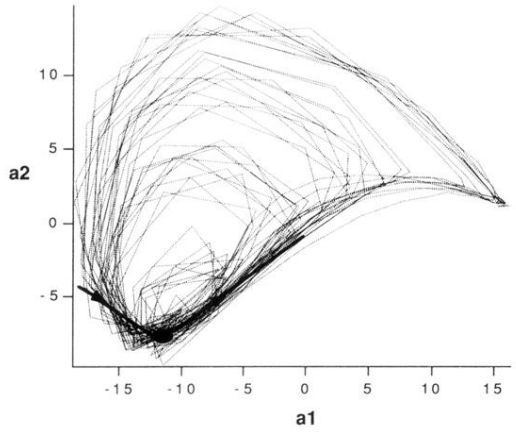

FIG. 1. Projected dynamics from the video tape in the phase space spanned by the first two Karhunen-Loeve modes. The fixed point $\mathbf{a}^*$ and its eigenvectors $\hat{\mathbf{e}}_1$ and $\hat{\mathbf{e}}_2$ are shown.